The Importance of Humidity Effect in Determining Flux-Profile Parameters of a Marine Surface Layer

ALOYSIUS KOUFANG LO

Modelling and Integration Research Division, Atmospheric Environment Service, Downsview, Ontario Canada

(Manuscript received 24 July 1995, in final form 1 November 1995)

ABSTRACT

The role of humidity in estimating marine surface layer stratification in terms of the ratio, R, of the humidity contribution to the total static stability is evaluated. A recent study of Geernaert and Larsen employs a system of simultaneous equations for calculating R. The present study requires only simple algebraic relations to arrive at the approximate solution of R. In the approximate solution, the value of R is explicitly represented in a single equation as a function of potential temperatures and the corresponding virtual potential temperatures. The exact solution of R is obtained directly using the Monin–Obukhov stability parameters with and without humidity effect. Static stability and transfer coefficients, as well as deposition velocity of SO_2 over an air–sea interface, are calculated using the direct bulk aerodynamic method similar to that of Lo. Detailed study on the characteristics of humidity effect on atmospheric stratification, especially for cases of large sea–air temperature differences under stable conditions, are presented. Implication of humidity effect on stability pertaining to the theory of "countergradient" phenomenon is also presented.

1. Introduction

Turbulent fluxes are known to play key roles in the energy transport mechanism of the atmosphere–ocean system and are essential to the understanding of the generation and transportation of aerosol and other impurities at the air–sea interface. Of particular importance to the study of air–sea interaction is the knowledge of atmospheric stratification of the marine boundary layer. Atmospheric stratification provides a measure of and relates to the direction of momentum, sensible heat, and latent heat flux transfer taking place. The momentum, sensible heat, and latent heat transfer collectively determine the state of stratification or the static stability of the atmosphere. Although the possible impact of humidity effect are well acknowledged (e.g., Blanc 1983; Smith 1988; Walmsley 1988), due to the unavailability of humidity measurements or merely for simplicity, that static stability is determined directly or indirectly considering only the contribution of temperature and velocity gradients. The humidity gradient, an equally important contributing factor, is often ignored. The fact that calculations based on velocity and temperature gradients alone can still yield satisfactory results are due to the high frequency of measurements conducted over relatively cool water bodies. Since air density depends on both temperature and humidity, a vertical upward gradient of either quantity can cause dynamic instability in the air parcel in question. Moreover, since virtual temperature represents a measure of the humidity content of the atmosphere, virtual temperature not potential temperature should be used for determining atmospheric stability, flux parameters, and transfer coefficients in a marine surface layer. This is especially so in the case of marine surface layers in proximity of a coastal area or over lake water bodies. The reasoning is that in contrast to the ocean air–sea interaction, the air–sea interaction in the coastal area is significantly affected by the presence of a land mass, particularly on marine aerosol. A similar argument can be made for lakes, except in the center of very large lakes, the marine boundary layer over most part of the lake surface is strongly stratified. This is due to the frequent occurrences of cold air inflow on to the warm lake surface or warm air onto the cold water surface. On the other hand, stratification over an ocean is almost always near-neutral, except in the coastal area. Covering vast distances over the homogeneous water surface, air in the near-water layer attains similar temperature to that of the ocean surface.

It is the purpose of this study to show the dramatic importance of humidity and humidity flux in a marine surface layer associated with coastal air–sea interactions, particularly over a warm water body.

2. Method of calculations

In the surface boundary layer where the Monin–Obukhov similarity theory applies, it is well known

Corresponding author address: Aloysius Koufang Lo, Modelling and Integration Research Division, Atmospheric Environment Service, Environment Canada, 4905 Dufferin Street, Downsview, ON M3H 5T4, Canada.

that the bulk Richardson number and the static stability are in one to one correspondence, and except under highly stable conditions are in a near-linear relationship (see, e.g., Fig. 1; Lo 1993). In other words, under most stability conditions, we can simply assume without loss of generality that $z/L)_v \propto \mathrm{Ri}_b)_V$ and $z/L)_T \propto \mathrm{Ri}_b)_T$. The bulk Richardson numbers $\mathrm{Ri}_b)_T$, excluding humidity effect, and $\mathrm{Ri}_b)_V$, including humidity effect, can be written as follows:

$$\mathrm{Ri}_b)_T = \frac{g}{T}\frac{(T_a - T_s)(z - z_{0m})^2}{(U_a - u_0)^2(z - z_{0h})}$$

$$\mathrm{Ri}_b)_V = \frac{g}{T_v}\frac{(T_{aV} - T_{sV})(z - z_{0m})^2}{(U_a - u_0)^2(z - z_{0h})}, \qquad (1)$$

where g is the acceleration of gravitation, z_{0h} and z_{0m} are roughness lengths for heat and momentum, T is the mean potential temperature, u_0 is the drift velocity, and subscripts a, s, and v indicate atmospheric, sea, and virtual temperatures. As an approximation, it is not unreasonable to further assume that R, representing the ratio of stability contribution due to moisture effect to the total static stability, can be expressed as

$$R = \frac{z/L)_V - z/L)_T}{z/L)_V} \approx \frac{\mathrm{Ri}_b)_V - \mathrm{Ri}_b)_T}{\mathrm{Ri}_b)_V}$$

or

$$R \approx 1 - \frac{(T_s - T_a)}{(T_{sV} - T_{aV})}\frac{T_V}{T}.$$

Since T_V and T are absolute temperatures in kelvins and have nearly the same values, it can be assumed that $T_V/T \approx 1$ and then

$$R \approx 1 - \frac{T_s - T_a}{T_{sV} - T_{aV}}, \qquad (2)$$

where $z/L)_V$ and $z/L)_T$ are stabilities including humidity effect and not including humidity effect, respectively. Virtual temperatures T_{sV} and T_{av} can be calculated from the empirical formula,

$$T_V = T(1. + 0.608q), \qquad (3)$$

where q is the specific humidity at the measuring height in question. When specific humidity is not measured, it can be estimated empirically from the saturation vapor pressure e_s at temperature T, pressure p, and the assumed relative humidity RH. And, as in Geernaert (1990),

$$q = q_s\mathrm{RH} \qquad (3a)$$

$$q_s = 0.622\frac{e_s}{p} \qquad (3b)$$

$$\ln(e_s) = A + B\left(\frac{1000}{T}\right) + C\left(\frac{1000}{T}\right)^2, \qquad (3c)$$

where RH for a marine surface layer is in the neighborhood of 60% to 75% for clear-sky conditions and the surface RH is assumed to be 100% with respect to water surface temperature. The saturation vapor pressure and air pressure are in milibars. The empirical constants are $A = 8.42926609$, $B = -1.82717843$, and $C = -0.071208271$. Knowing the virtual potential temperatures, exact values of R, z/L, transfer coefficients C_d and C_h, and the deposition velocity of SO_2 can be evaluated using the direct bulk aerodynamic method similar to that of Lo (1993, 1996, submitted to *Atmos. Environ.*). As given in Lo (1996, submitted to *Bound.-Layer Meteor.*) and also reproduced in the appendix, the relationships of ζ as a function of Ri_b are as follows:

For the stable case,

$$\zeta = \frac{z}{z - z_{0m}}\frac{-B - (B^2 - 4AC)^{1/2}}{2A} \qquad (4)$$

where

$$A = \Pi\left(\frac{\mathrm{Ri}_b}{\mathrm{Pr}_0}\beta_m^2 - \beta_h\right)$$

$$B = 2\Pi\,\mathrm{Ri}_b\beta_h \ln\frac{z}{z_{0m}} - \ln\frac{z}{z_{0h}}$$

$$C = \frac{\mathrm{Ri}_b}{\mathrm{Pr}_0}\Pi\left(\ln\frac{z}{z_{0m}}\right)^2$$

and

$$\Pi = \frac{z - z_{0h}}{z - z_{0m}}.$$

Equation (4) becomes identical to Eq. (19) of Byun (1990) when $z_{0h} = z_{0m}$ is assumed. For the unstable case,

$$F(\zeta; \mathrm{Ri}_b) = \frac{\mathrm{Ri}_b}{\mathrm{Pr}_0}\frac{z}{z - z_{0m}}\Pi\left(\ln\frac{z}{z_{0m}} - \psi_m\right)^2 - \left(\ln\frac{z}{z_{0h}} - \psi_h\right)\zeta = 0. \qquad (5)$$

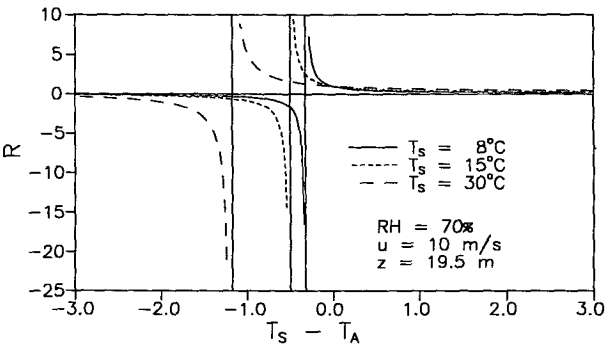

FIG. 1. Approximate ratio of stability contribution due to humidity effect to total static stability, from Eq. (2).

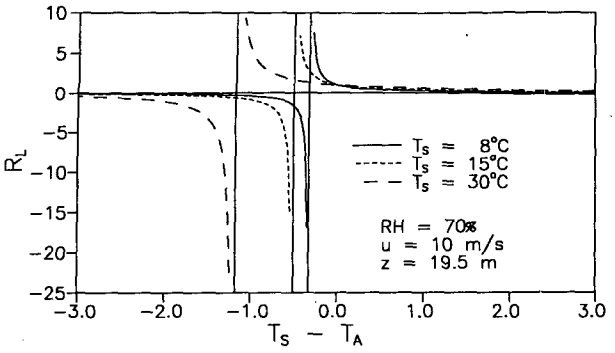

FIG. 2. Exact ratio of stability contribution due to humidity effect to total static stability, from Eq. (6).

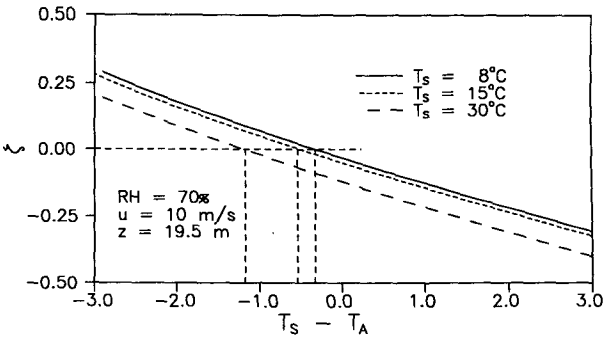

FIG. 3. Variations of static stability as a function of sea–air temperature difference.

Equation (5) can easily be solved by numerical iterations using

$$\zeta = \frac{z}{z - z_{0m}} \ln\left(\frac{z}{z_{0m}}\right) \mathrm{Ri}_b$$

as an initial value, where $\mathrm{Pr}_0 = 0.74$ is the turbulent Prandtl number, β_m, β_h, γ_m, γ_h are empirical constants according to Businger et al. (1971), $\beta_m = 4.7$, $\beta_h = 6.35$, $\gamma_m = 15$, $\gamma_h = 9$, and the integrated diabatic influence functions are

$$\psi_m = 2 \ln\left(\frac{1 + x}{1 + x_0}\right) + \ln\left(\frac{1 + x^2}{1 + x_0^2}\right) - 2 \tan^{-1}(x) + 2 \tan^{-1}(x_0)$$

$$\psi_h = 2 \ln\left(\frac{1 + y}{1 + y_0}\right),$$

where $\zeta_{0m} = z_{0m}/L$, $\zeta_{0h} = z_{0h}/L$, L is the Monin–Obukhov length, and

$$x = \left[1 - \gamma_m\left(\frac{z}{L}\right)\right]^{1/4}, \quad x_0 = \left[1 - \gamma_m\left(\frac{z_{0m}}{L}\right)\right]^{1/4},$$

$$y = \left[1 - \gamma_h\left(\frac{z}{L}\right)\right]^{1/2}, \quad y_0 = \left[1 - \gamma_h\left(\frac{z_{0h}}{L}\right)\right]^{1/2}.$$

The static stabilities including and not including humidity effect, $\zeta_V = z/L)_V$ and $\zeta_T = z/L)_T$, can be determined using the corresponding virtual potential temperatures and potential temperatures in (3), (4), and (5), respectively. Knowing $z/L)_V$ and $z/L)_T$, the value R representing a ratio of stability due to humidity contribution to the total static stability can then be calculated from

$$R_L = \frac{z/L)_V - z/L)_T}{z/L)_V}, \tag{6}$$

where subscript L indicates calculation of the R value directly from the ratio of stabilities to differentiate with R in (2). To demonstrate the significance of humidity effect on static stability, which in turn will alter boundary layer and other related parameters, we calculate the transfer coefficients C_d and C_h, and the dry deposition velocity of SO_2, V_d as follows:

$$C_d)_{V,T} = \left.\frac{u_*^2}{u^2}\right)_{V,T}$$

$$C_h)_{V,T} = \left.\frac{u_* T_*}{u(T_s - T)}\right)_{V,T}, \tag{7}$$

and as in Lo (1996)

$$V_d = \frac{\kappa u_*}{\left[\ln\dfrac{z}{z_c} - \psi_c\left(\dfrac{z}{L}\right)\right]_{V,T}},$$

where subscripts v, T refer to calculation based on virtual and potential temperature, respectively. Term u_* is the friction velocity, $z_c = D_c/\kappa u_*$ is the capture length, D_c is the molecular diffusivity for SO_2, $\kappa = 0.4$ is the von Kármán constant and $\psi_c(z/L)$ is the integrated diabatic influence function for the contaminant SO_2 and is assumed to have the same functional form of $\psi_h(z/L)$, the integrated diabatic influence function for heat.

TABLE 1. Comparison of R values calculated from Eq. (2) to that calculated from Eq. (6) at various values of $T_s - T_a$ for $T_s = 15$°C.

$T^w - T_a$	−1.0	−0.9	−0.8	−0.7	−0.6	−0.5	−0.4	−0.3	−0.2	−0.1	0.0	0.1	0.2	0.3	0.4	0.5
R	−0.85	−1.09	−1.49	−2.31	−4.84	80.49	4.47	2.34	1.60	1.23	1.00	0.85	0.74	0.66	0.59	0.54
R_L	−0.91	−1.15	−1.56	−2.40	−5.02	83.02	4.58	2.39	1.62	1.23	1.00	0.85	0.73	0.65	0.59	0.53

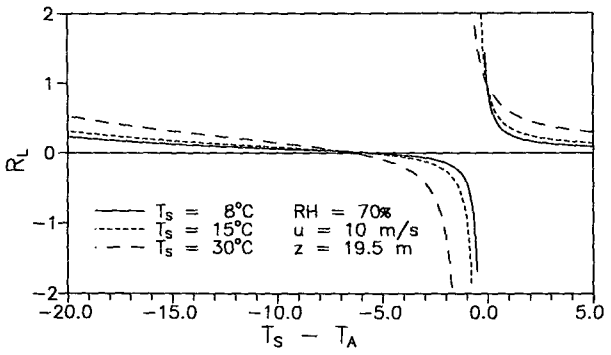

FIG. 4. Ratio of stability contribution due to humidity effect to total static stability, calculated to $T_s - T_a = 20°C$.

That is,

$$\psi_c\left(\frac{z}{L}\right) = \psi_h\left(\frac{z}{L}\right) = -\beta_h(\zeta - \zeta_c) \quad \text{for} \quad \zeta > 0$$

and

$$\psi_c\left(\frac{z}{L}\right) = \psi_h\left(\frac{z}{L}\right) = 2\ln\left(\frac{1+y}{1+y_c}\right) \quad \text{for} \quad \zeta > 0,$$

with

$$y = (1 - \gamma_h\zeta)^{1/2}, \quad y_c = (1 - \gamma_h\zeta_c)^{1/2}, \quad \zeta_c = \frac{z_c}{L}.$$

Here the choice of SO_2 is strictly based on its unique physical property. The choice of any other gas will not be as meaningful for the purpose of this study. The reasons are as follows: SO_2 and a few other gases such as NH_3, HNO_3, H_2O etc., are highly reactive and soluble in water. In essence, SO_2 has a very low Henry's law constant. The air–water transfer process of SO_2 is thus dominated by the air-phase resistance in that $r_a \gg r_w$, the water-phase resistance. Consequently, any change in the turbulent properties of the air layer will automatically be reflected in r_a and hence in deposition velocity. In other words, the deposition velocity of SO_2 is very sensitive to errors of surface-layer parameters and errors in surface-layer parameters will be fully reflected in the deposition velocity of SO_2. In contrast, this is not the case for other gases with $r_w \gg r_a$ for which the transfer process is dominated by water resistance. Variations in the surface-layer properties contribute very little changes to the total resistance and, hence, very little changes in the deposition velocity.

3. Results and discussions

To facilitate comparison, calculations were based on exactly identical meteorological conditions to those of Geernaert and Larsen (1993). Specifically, relative humidity of air is assumed to be 70%, wind speed at the measurement height of 19.5 m is 10 m s^{-1}, $\alpha = 0.012$ is assumed in Charnock's formula, $z_0 = \alpha u_*^2/g$, for the roughness length associated with the wind profile, and, as in Geernaert and Larsen, the roughness length for heat, z_{0h}, is assumed to be 8.3×10^{-6} m. Typical sea surface temperatures of 8°, 15°, and 30°C were chosen. Estimations for R are made using the simplistic equation (2) involving only the ratio of virtual potential temperature difference to the corresponding potential temperature difference. Results are shown in Fig. 1. A striking resemblance to Fig. 1 of Geernaert and Larsen can be observed. However, upon closer examination, it is found that vertical asymptotes for SST = 8°, 15°, and 30°C exist at $\Delta T = T_s - T_a = -0.3°$, $-0.5°$, and $-1.2°C$, respectively, using our method in comparison

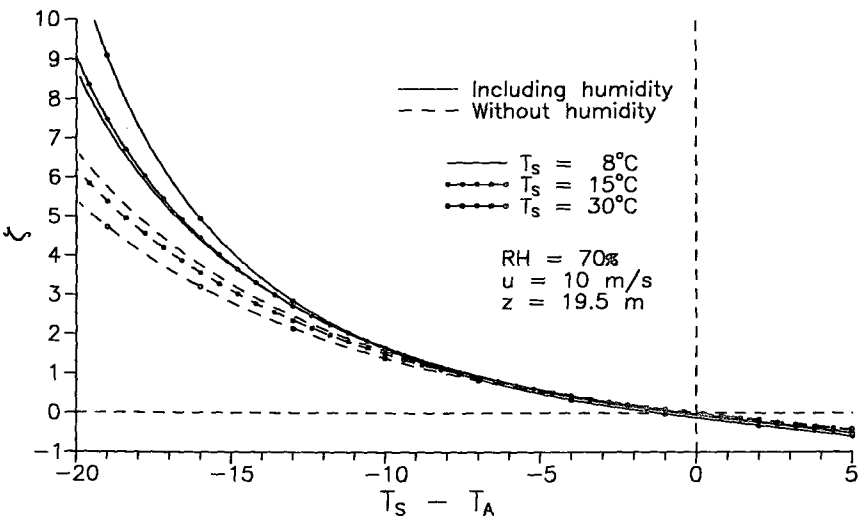

FIG. 5. Variation of static stability as a function of sea–air temperature difference to $T_s - T_a = 20°C$.

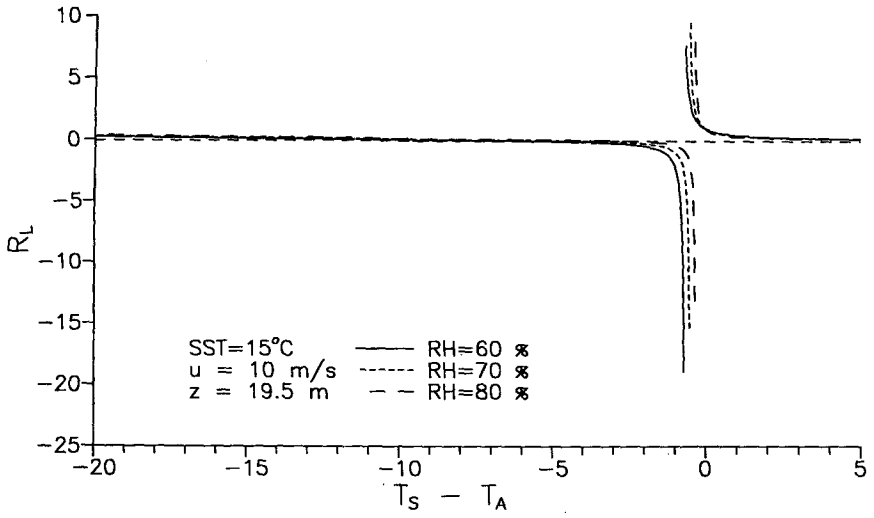

FIG. 6. Effect or relative humidity on ratio R as a function of sea–air temperature difference at T_s = 15°C = const.

to −0.5°, −0.8°, and −2.0°C, respectively, in Fig. 1 of Geernaert and Larsen. Our initial interpretation is that this marked difference might be a result of the approximation used to arrive at (2). We then proceed to calculate the more exact result for R_L based on flux profile equations of the similarity theory analogous to those used in Geernaert and Larsen. While Geernaert and Larsen's (1993) calculation requires a set of 24 equations, including several simultaneous transcendental equations, the present calculation employs the much simpler direct method similar to that of Lo (1993). Figure 2 represents result of R computed from the exact equation (6) is almost indistinguishable compared to Fig. 1 from (2). This near-perfect agreement between Figs. 1 and 2 provides us with a measure of confidence such that (6) can be approximated by the corresponding Richardson numbers that, in turn, can be expressed in terms of potential and virtual potential temperatures. To further verify this, Table 1 presents R and R_L values for the case T_s = 15°C from both (2) and (6) at the most sensitive range of sea–air temperature differences around −0.5°C where the vertical assymptote exists. The discrepancy between these two R values are well within a few percents, except for highly stable cases with $\mathrm{Ri}_b \geq 0.2$. For $\mathrm{Ri}_b \geq 0.2$, turbulence is greatly suppressed and the Monin–Obukhov similarity theory

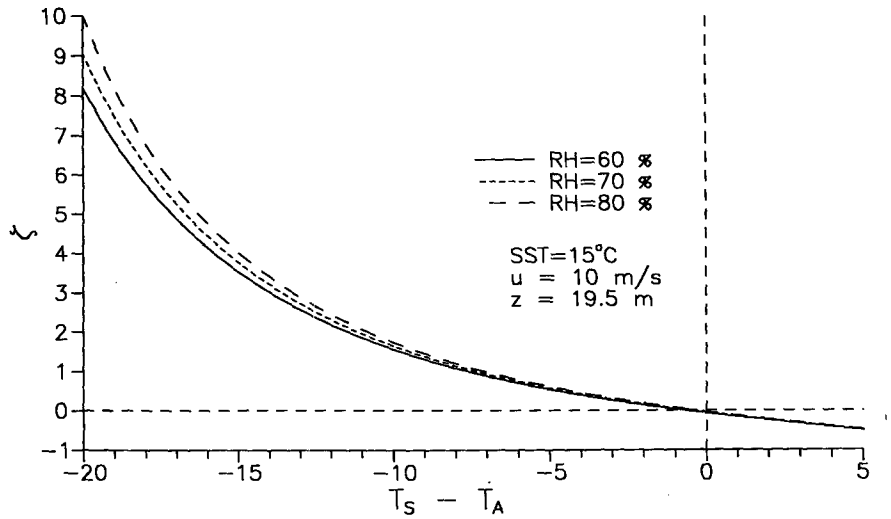

FIG. 7. Effect of relative humidity on stability as a function of sea–air temperature difference at T_s = 15°C = const.

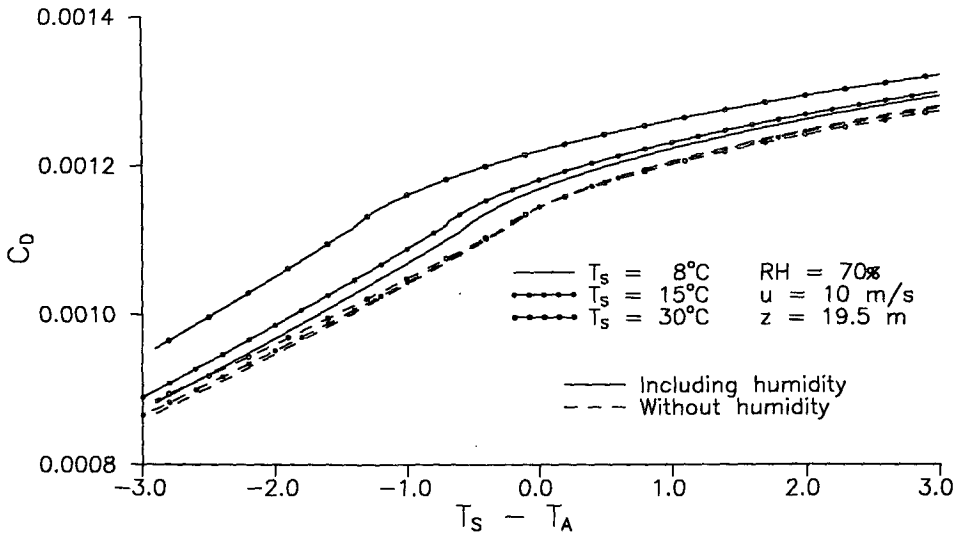

FIG. 8. Variation of drag coefficient as a function of sea–air temperature difference with and without humidity effect.

becomes less applicable at such large Ri_b values. In fact, as Ri_b approaches the value 0.2, the ζ versus Ri_b curve deviates rapidly from near-linear shape to that with a very large curvature. For still larger Ri_b values, the ζ versus Ri_b solution breaks down due to multiple values of ζ at $Ri_b > 0.2$. This is due to the fact that beyond $Ri_b \approx 0.2$, the empirical constants of Businger et al. and the Monin–Obukhov similarity theory are no longer valid. It is to be noted that in both Figs. 1 and 2, vertical asymptotes for R exist at $\Delta T = -0.3°$, $-0.5°$, and $-1.2°C$, where the total static stability approaches zero while the contribution due to the humidity effect is nonzero. These are the sea–air temperature differences at which the atmosphere is neutrally stratified. That is, when z/L approaches 0, R approaches ∞ and the humidity contribution to z/L becomes dominant. Also, as noted in Geernaert and Larsen (1993) for warmer SSTs, the importance of the humidity effect to atmospheric stability substantially increases in the increasing negative regions of ΔT away from the vertical assymptotes and for positive values of sea–air temperature differences. At lower SST the humidity effect is small and large values of R are very close to the origin near $\Delta T = 0$. Humidity effect increases with increasing

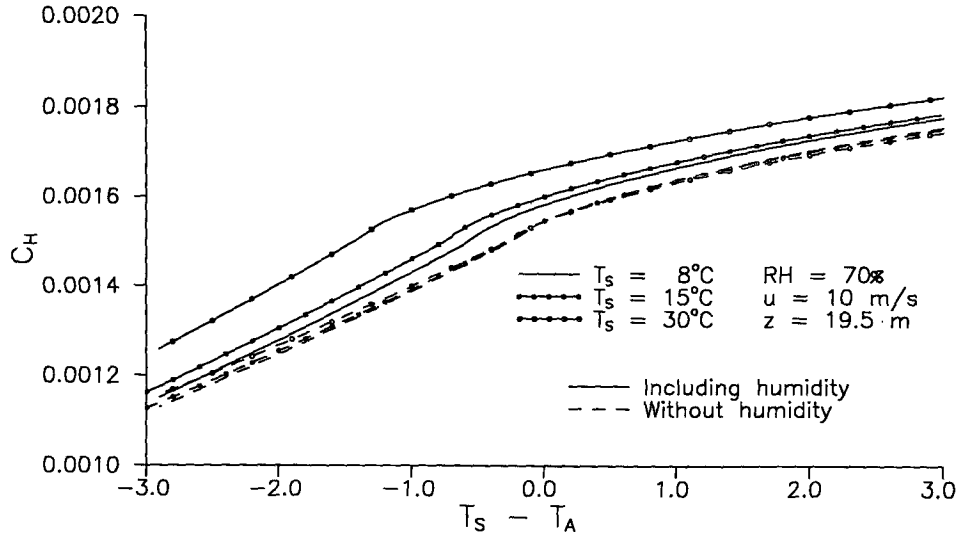

FIG. 9. Variation of heat transfer coefficient as a function of sea–air temperature difference with and without humidity effect.

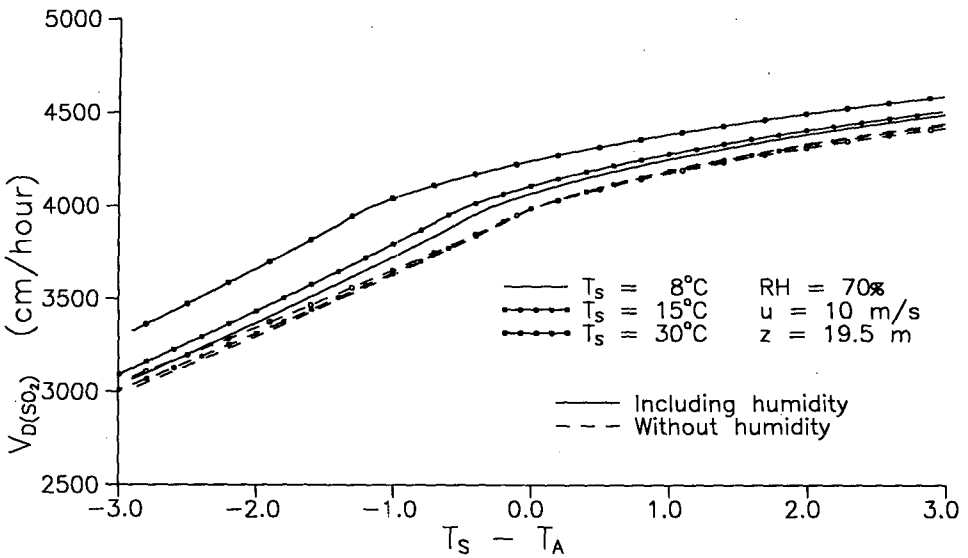

FIG. 10. Variation of dry deposition velocity of SO_2 as a function of sea–air temperature difference with and without humidity effect.

SST, and large values of R shift toward more negative ΔT. Alternately, this can be interpreted as humidity effect increasing the instability in the unstable region, therefore shifting the neutral stability point to negative ΔT away from the origin where $\Delta T = 0$. Within the stable region, the humidity effect increases the stability with increasing ΔT. To further demonstrate the humidity effect on stability, variations of stability with ΔT for SST = 8°, 15°, and 30°C are shown in Fig. 3. We note that in each case, positions of $\zeta = 0$ are displaced from the origin where $\Delta T = 0$. The increasing negative value of sea–air temperature difference at which $\zeta = 0$ are $\Delta T = -0.3$, -0.5°, and -1.2°C for increasing warmer SST = 8°, 15°, and 30°C, respectively. They correspond to locations of vertical asymptotes in Figs. 1 and 2. These ΔT differences show that in the absence of humidity measurement and for most practical range of sea–air potential temperature differences, the approximate equation (2) derived in the present study in terms of temperature difference alone can constitute an accurate method for evaluating humidity effect over stratification. Figure 3 of the present study shows three rather smooth lines with slight concave curvatures. Figure 2 of Geernaert and Larsen shows three curves with slight wiggle prior to curving sharply upward at sea–air temperature difference beyond −2°C. It is not clear to us why the present results on the position of vertical asymptotes or the dislocated positions of the neutral stability differs from that of Geernaert and Larsen. We also feel that the near-straight linear shape of smooth curves in Fig. 3 of the present study is what one would expected from the relation between ζ and sea–air temperature differences (see, e.g., ζ versus ΔT without humidity effect). Since both the present study and that of Geernaert and Larsen are based on fundamentally similar sets of flux-profile equations, results of similar nature but somewhat different in values seem to be puzzling. We see one difference in calculation is that Geernaert and Larsen assumed roughness length for moisture as $z_{0q} = 2.1 \times 10^{-4}$ m, while the present study z_{0q} is not required. Uncertainties in the value of z_{0q} can contribute appreciable discrepancy to related calculations since it is the case for z_{0h} (e.g., Lo 1996, submitted to *Bound.-Layer Meteor.*). Another possible source of error is that values of bulk transfer coefficients for fluxes of momentum, sensible heat, and latent heat C_d, C_h, and C_e in Geernaert and Larsen are obtained either from look-up tables (Smith 1988) or by using analytical formulations (Geernaert 1990). Any discrepancy in evaluating the transfer coefficients can generate errors in subsequent calculations and hence introduce error in R and ζ. The present study employs the calculation procedure of the direct bulk aerodynamic method of Lo (1993). Values of transfer coefficients, C_d, C_h, as well as other boundary layer parameters, need not be given or precalculated. They are part of the solution and thus eliminates any possible errors. It is to be pointed out again that in Fig. 2 of Geernaert and Larsen, all three curves veer sharply upward, indicating a tendency to approach infinity assymptotically at about $\Delta T = -2.5$°C. At that sea–air temperature difference, $\mathrm{Ri}_b = 0.015$ is well within the range where the Monin–Obukhov similarity theory applies. And ζ curve should, in principle, still be relatively smooth and its value remain in bound. It is therefore felt that results of Geernaert and Larsen may require further confirmation. It is to be noted that results in Figs. 1, 2 and 3 of the present study and the

corresponding figures in Geernaert and Larsen terminated calculations at about $\Delta T = -3$°C. To further examine the ζ versus ΔT relationship, we have extended our calculations to higher negative values of ΔT. As shown in Figs. 4 and 5, in the unstable region, the humidity effect increases the ΔT range to which unstable atmosphere prevails. In other words, the point of neutral stability is being displaced toward negative ΔT region. In contrast, within the stable region, the humidity effect at first makes the atmosphere less stable until at a certain ΔT at which the humidity effect reverses its role to rapidly increases the stability of the atmosphere. At a still higher negative sea–air temperature difference of $\Delta T \approx 10$°C, water bodies with lower SST become increasingly more stable than those of higher SST. Although it may not be realistic for the case of SST = 30°C to have a sea–air temperature difference of −10° to −20°C, it is reasonable for cases of SST = 8°C and may even be plausible for SST = 15°C to exist under such a large sea–air temperature difference. Conditions like these are not uncommon over parts of the Atlantic Ocean and especially over the Great Lakes during the summer seasons. The above contrasting phenomena becomes more pronounced under conditions of higher SST while RH is kept constant, or lower RH while T_s is kept constant, as shown in Figs. 6 and 7. That is, both higher T_s or lower RH have the same effect on atmospheric stability under most sea–air temperature differences. Figures 8, 9, and 10 show the difference of C_d, C_h, and V_d of SO_2 with and without humidity effect under condition of three SST of 8°, 15°, and 30°C. The discrepancy of results between these two families of curves with and without humidity effect are rather appreciable. This discrepancy reflects the propagation of the humidity effects into calculations of fluxes and other stability-dependent parameters. The largest discrepancy occurs at the point of dislocated neutral stability. This is consistent with earlier findings where the humidity contribution becomes a dominant factor at dislocated points of neutral stability. By definition, the virtual temperature is a measure of the humidity contents of the atmosphere. Therefore, it can be said that under the combined conditions of warmer water temperature, larger sea–air temperature difference, and lower atmosphere RH, the atmospheric stratifications are heavily influenced by the humidity content. Hence, stratification may be due equally to the latent heat flux as well as to the sensible heat flux.

4. Conclusions

The contribution of humidity to the total static stability is expressed in terms of a ratio, R. In the present study, R is first derived using the near-linear relationship between the bulk Richardson number and its corresponding static stability to arrive at a very simple equation:

$$R = 1 - \frac{T_s - T_a}{T_{sV} - T_{aV}}.$$

Detailed calculations are based on the direct method similar to that of Lo (1993). Essential equations are those providing the relationships between the Monin–Obukhov stability and the bulk Richardson number. Results of R calculated from the approximate equation (2) agree exceptionally well in comparison to the exact equation (6) in detailed calculations. Therefore, (2), with its simplicity, will be very useful for carrying out in situ evaluations of humidity effect during a marine boundary layer expedition. Both R and the total static stability results of the present study bear remarkable resemblance to those of Geernaert and Larsen (1993). It is to be pointed out here that the present approach of the direct method is extremely simple, using straightforward calculations as compared to that of Geernaert and Larsen. The extent of dislocations of the neutral stability from the origin $T_s - T_a = 0$ is somewhat less in the results of the present study compared to those of Geernaert and Larsen. Humidity effect on transfer coefficients and on the dry deposition velocity of SO_2 are found to be significant, especially over warmer water body. It is concluded that in dealing with a marine surface layer, calculations of static stability and other marine surface layer parameters ought to take humidity effect into account by using virtual potential temperature instead of potential temperature.

It is also our belief that the displacement of the neutral stability point due to humidity effect may contain another profoundly important meaning. In the case of SST = 15°C in Fig. 3, for example, the displaced neutral stability point is at $\Delta T = -0.5$°C. The domain between $\Delta T = 0$°C and $\Delta T = -0.5$°C that was originally deemed stably stratified is now unstably stratified. In other words, without considering the humidity effect, there would have existed an area where the gradient of T exhibits a direction opposite to that of the flux under unstable conditions. This is commonly known as the peculiar "countergradient" phenomenon. It now becomes clear, at least in the present case, that the so-called countergradient phenomenon becomes very explainable. In fact, we feel that the countergradient phenomenon may be a misconception, one that arises if and only if stratification is defined with respect to the potential temperature gradient. The countergradient phenomenon may become nonexistant if the humidity effect has been rightfully taken into consideration and the flux-gradient relationship is defined in terms of the virtual potential temperature gradient.

APPENDIX

Relationship between the Monin–Obukhov Stability Parameter and the Bulk Richardson Number

Based on Monin–Obukhov similarity hypothesis, the flux-profile relationships are

$$U - u_0 = \frac{u_*}{\kappa}\left[\ln\left(\frac{z}{z_{0m}}\right) - \psi_m(\zeta, \zeta_{0m})\right] \quad \text{(A1)}$$

$$\Delta\theta = \theta - \theta_0 = \mathrm{Pr}_0\frac{\theta_*}{\kappa}\left[\ln\left(\frac{z}{z_{h0}}\right) - \psi_h(\zeta, \zeta_{0_h})\right], \quad \text{(A2)}$$

where Pr_0 is the turbulent Prandtl number = 0.74, κ = 0.4 is the von Kármán constant, u_* is the friction velocity, θ_* is the scaling temperature, z_{0m}, z_{0h} are the roughness lengths for momentum and heat, respectively, and the stability parameters are

$$\zeta = \frac{z}{L} = \frac{\kappa z g \theta_*}{\theta_0 u_*^2} \quad \text{(A3)}$$

$$\mathrm{Ri}_b = \frac{g}{\theta_0}\frac{\Delta\theta(z - z_{0m})^2}{(U - u_0)^2(z - z_{0h})}. \quad \text{(A4)}$$

If we use the functional forms for the flux-profile relationships of Businger et al. (1971), Ψ_m and Ψ_h are the integrated diabatic influence functions and can be integrated to give the following forms.

For the stable case

$$\psi_m = -\beta_m(\zeta - \zeta_{0m})$$
$$\psi_h = -\beta_h(\zeta - \zeta_{0h}). \quad \text{(A5)}$$

For the unstable case,

$$\psi_m = 2\ln\left(\frac{1 + x}{1 + x_0}\right) + \ln\left(\frac{1 + x^2}{1 + x_0^2}\right) - 2\tan^{-1}(x) + 2\tan^{-1}(x_0)$$

$$\psi_h = 2\ln\left(\frac{1 + y}{1 + y_0}\right), \quad \text{(A6)}$$

where $\zeta_{0m} = z_{0m}/L$, $\zeta_{0h} = z_{0h}/L$, L is the Monin–Obukhov length, and

$$x = \left[1 - \gamma_m\left(\frac{z}{L}\right)\right]^{1/4}, \quad x_0 = \left[1 - \gamma_m\left(\frac{z_{0m}}{L}\right)\right]^{1/4},$$
$$y = \left[1 - \gamma_h\left(\frac{z}{L}\right)\right]^{1/2}, \quad y_0 = \left[1 - \gamma_h\left(\frac{z_{0h}}{L}\right)\right]^{1/2}.$$

The empirically determined constants as given by Businger et al. (1971) are $\beta_m = 4.7$, $\beta_h = \beta_m/\mathrm{Pr}_0 = 6.35$, $\gamma_m = 15$, and $\gamma_h = 9$.

For the stable case, we use (A1)–(A5) and after some algebra one can obtain

$$\zeta = \frac{z}{z - z_{0m}}\frac{-B - (B^2 - 4AC)^{1/2}}{2A}, \quad \text{(A7)}$$

where

$$A = \Pi\left(\frac{\mathrm{Ri}_b}{\mathrm{Pr}_0}\beta_m^2 - \beta_h\right)$$

$$B = 2\Pi\,\mathrm{Ri}_b\beta_h\ln\frac{z}{z_{0m}} - \ln\frac{z}{z_{0h}}$$

$$C = \frac{\mathrm{Ri}_b}{\mathrm{Pr}_0}\Pi\left(\ln\frac{z}{z_{0m}}\right)^2$$

and

$$\Pi = \frac{z - z_{0h}}{z - z_{0m}}.$$

Equation (A7) becomes identical to Eq. (19) of Byun (1990) when $z_{0h} = z_{0m}$ is assumed.

For the unstable case, we use (A1)–(A4) and (A6), and after some algebra, we arrive at a nonlinear transcendental equation in ζ and Ri_b:

$$F(\zeta; \mathrm{Ri}_b) = \frac{\mathrm{Ri}_b}{\mathrm{Pr}_0}\frac{z}{z - z_{0m}}\Pi\left(\ln\frac{z}{z_{0m}} - \psi_m\right)^2 - \left(\ln\frac{z}{z_{0h}} - \psi_h\right)\zeta = 0. \quad \text{(A8)}$$

Equation (A8) can easily be solved by numerical iterations using

$$\zeta = \frac{z}{z - z_{0m}}\ln\left(\frac{z}{z_{0m}}\right)\mathrm{Ri}_b$$

as an initial value.

REFERENCES

Blanc, T. V., 1983: Typical influences of moisture on profile measurements in the marine atmospheric surface layer. *Bound.-Layer Meteor.*, **25,** 411–415.

Byun, D. W., 1990: On the analytical solutions of flux-profile relationships for the atmospheric surface layer. *J. Appl. Meteor.*, **29,** 652–657.

Geernaert, G. L., 1990: Bulk parameterizations for the wind stress and heat flux. *Surfaces Waves and Fluxes: Theory and Remote Sensing,* Vol. 1, G. Geernaert and W. Plant, Eds., Kluwer, 91–172.

——, and S. Larsen, 1993: On the role of humidity in estimating marine surface layer stratification and scatterometer cross section. *J. Geophys. Res.* **98** (C1), 927–932.

Lo, A. K., 1993: The direct calculation of fluxes and profiles in the marine surface layer using measurements from a single atmospheric level. *J. Appl. Meteor.*, **32,** 1890–1990.

Smith, S. D., 1988: Coefficients for sea surface wind stress, heat flux, and wind profiles as a function of wind speed and temperature. *J. Geophys. Res.*, **93,** 15 467–15 472.

Walmsley, J. L., 1988: On theoretical wind speed and temperature profiles over the sea with applications to data from Sable Island, Nova Scotia. *Atmos.–Ocean,* **26**(2), 203–233.